Self-forcing Mechanism of the Braided Tube as a Robotic Gripper

Zufeng Shang
Key Lab for Mechanism Theory and Equipment Design of Ministry of Education, Tianjin University, Tianjin 300354, China
e-mail: szf_rai@tju.edu.cn

Jiayao Ma[1]
Key Lab for Mechanism Theory and Equipment Design of Ministry of Education, Tianjin University, Tianjin 300354, China
e-mail: jiayao.ma@tju.edu.cn

Jinhua Li
Key Lab for Mechanism Theory and Equipment Design of Ministry of Education, Tianjin University, Tianjin 300354, China
e-mail: lijinhua@tju.edu.cn

Zemin Zhang
Key Lab for Mechanism Theory and Equipment Design of Ministry of Education, Tianjin University, Tianjin 300354, China
e-mail: zmzhang0526@tju.edu.cn

Guokai Zhang
Key Lab for Mechanism Theory and Equipment Design of Ministry of Education, Tianjin University, Tianjin 300354, China
e-mail: zhang_gk@tju.edu.cn

Shuxin Wang[1]
Key Lab for Mechanism Theory and Equipment Design of Ministry of Education, Tianjin University, Tianjin 300354, China
e-mail: shuxinw@tju.edu.cn

ABSTRACT

Gripper, which acts as the end effector and contacts the objects directly, has great effects on the robotic performance. Braided tube is a kind of structure with great deployability. In this paper, we find that the braided tube exerts excellent self-forcing mechanism, for which the holding force is enhanced with the increase of the load/object weight. The mechanism together with the deployability facilitates grasping objects with different shapes, weights, and rigidities of the braided tube as a robotic gripper. Taking a

[1] Joint corresponding authors.

cylindrical object as an example, the self-forcing mechanism is theoretically analyzed, and explicit formulas are established to estimate the holding force range. Experimental and numerical analyses are also conducted for a more detailed understanding of the mechanism. The results show that a 1.2 time holding force increment of the tested gripper is obtained for the self-forcing, and the holding force can be further improved with a suitable parameter selection. In addition, a braided gripper is fabricated and mounted on a KUKA robot arm, and successfully grasps the fragile and the deformable objects. All these show the great promise of the braided tube as the robotic gripper.

Key words: *self-forcing mechanism, braided tube, robotic gripper, holding force, deployability*

1. INTRODUCTION

Gripper is an important kind of end effector mounted on the end of the manipulator to provide robots with the capacity of accomplishing a wide variety of manipulative assignments [1]. The gripper greatly affects the functionalities of the robots for it contacts the objects directly [2]. Conventional rigid-bodied grippers are always with limited adaptability, making them easy to drop or crush the objects [3]. In recent years, soft grippers have become one of the main research areas for their great advantages in adaptability over the rigid ones. Considering the unpredictable or inconsistent properties of the objects, an effective soft gripper needs to be universal, i.e., to be able to grasp objects with various shapes, weights, rigidities and so on [2, 4].

To achieve universal grasping, various promising grippers have been designed. One popular group is anthropomorphic hand with two or more articulated fingers [5, 6]. This gripper resembles human hand the most, which exerts great dexterity to grasp objects with different shapes and volumes. However, the high mechanical and control complexity, and difficulties in handling soft and deformable objects are great challenges [4, 7]. Recently, grippers with soft elements as the fingers to replace the articulated ones have

appeared [8, 9]. With the soft contacting, the fingers can bend around the object to pick it up with less damage. But insufficient force and difficulties in controlling the force are always the appendixes [4]. A step forward, underactuation has been adopted, making the hand fingers adaptive yet powerful [10, 11]. In addition to the hand-like grippers, grasping using controlled adhesion by electroadhesion or dry adhesive is also a promising method [12, 13]. It obtains great dexterity and versatility for its special grasping mechanism, allowing it to accomplish the most challenging tasks: grasping fragile, flat, soft and deformable objects. Also, it has some limitations, such as requirements for clean, relatively smooth and dry surfaces [4]. Granular jamming gripper is also a famous one for its high compliance [14, 15]. Its base is a bag containing granular coffee beans. It is soft at normal state, and turns to be rigid when the negative pressure is applied. With this mechanism, it can grasp various objects contributed by one or more of static friction, geometric constraints and vacuum suction [14]. It is easily controlled, and shows great superiorities in universal grasping. But it needs to partially envelop the object for grasping, and the holding force may be insufficient at a small gripper volume.

Braided tube is a kind of deployable structure, which is made of fibers interwoven in a crisscross pattern to form a tubular mesh configuration [16]. It shows desirable features including light weight, excellent flexibility, fatigue resistance and dimensional stability [17], and has been applied in various areas, such as piping industry [18, 19], soft robotics [20, 21], smart materials [22, 23] and medicine [24, 25]. Mechanical behaviours of the braided tube are of great importance and have been extensively studied. With the open-coiled spring theory [26], Jedwab and Clerc [27] analyzed the deployability and radial stiffness of the braided tube, and derived theoretical formulas to determine them. Radial

stiffness of the braided tube was also experimentally investigated by Wang et al [28] and numerically studied by Ni et al [29], which provided more validation to the theoretical analysis. Besides, Kim et al [30] studied the bending behaviour of the braided tube with numerical methods, and the results demonstrated the excellent flexibility of the structure. Li et al [31] designed a novel surgical instrument based on the braided tube, and proposed a simplified model to describe its binding capability.

In this paper, we find the braided tube exerts self-forcing mechanism, which contributes the tube to be a universal gripper. Its deployability helps to contain objects with a wide range of sizes and shapes, and the self-forcing mechanism, for which the holding force increases with the load, guarantees a higher holding force exerted while lifting heavy objects, and no excessive force to the light and fragile/deformable objects for no crushing. Obtaining the design tailorability, light weight, easy fabrication and control system, the gripper shows great promise especially in repetitively grasping objects with unpredictable properties. This paper focuses on the analysis of the self-forcing mechanism of the braided gripper and showing its feasibility, and the paper is organized as follows. In Section 2, the deployability of the braided gripper is firstly theoretically described. Besides, cylindrical object is taken as the example to theoretically explain the self-forcing mechanism, and explicit formulas are established to calculate the range of holding force. Next, experimental setup and the finite element modelling for the mechanism of the gripper are presented in Section 3. Subsequently are the results and discussions in Section 4. Finally, conclusion is given in Section 5 which ends the paper.

2. Theoretical analysis

2.1 Mechanism of the grasping

The braided gripper is made of spiral fibers interwoven in a crisscross pattern to form a tubular mesh configuration. Geometry of the braided gripper is shown in Fig. 1, which is determined by d, n, β, D and L. Other parameters, including p, c, D_i and D_o, are also commonly used, and can be calculated with the former five basis parameters.

$$\begin{cases} p = \pi D \tan\beta \\ c = L / p \\ D_i = D - 2d \\ D_o = D + 2d \end{cases} \tag{1}$$

Grasping mechanism of the braided gripper is illustrated in Fig. 2. First, the gripper exerts a smaller diameter to the grasped object. Next, drive the gripper to deploy (details in Section 2.2) to a larger profile with transmission wires. Then, move the gripper to contain the object. Finally, relax the transmission wire; the gripper will grasp the object automatically, and the object can be lifted for the self-forcing mechanism (details in Section 2.3). With the deployability and self-forcing mechanism, the object seems to be very suitable to grasp a wide range of objects with various shapes, rigidities and weights.

2.2 Deployability

Each fiber of the braided gripper is a helix, and spreading of one fiber in plane is shown in Fig. 3. For its large β, L and D will change obviously at the action of longitudinal load, leading to the gripper folding and deploying. Since the fiber is nearly inextensible, the fiber length remains unchanged during deformation and can be calculated by

$$l = c\pi D / \cos\beta = c\pi D' / \cos\beta' \tag{2}$$

where parameters of the deformed gripper are denoted with a prime. Simplifying Eq. (2), diameter of the deformed gripper can be acquired as

$$D' = D\cos\beta'/\cos\beta \tag{3}$$

β' theoretically ranges between 0° and 90° during deformation. A braided gripper can be fabricated at a slim state with a large β' approximate to 90°. In this state, the fibers huddle together, and the gripper diameter is about 2*d*. When β' tends to 0°, diameter of the gripper comes to its upper limit $D/\cos\beta$, which helps to form a large profile to contain objects with various shapes.

2.3 Self-forcing mechanism

Li et al. [31] proposed a simplified model to describe the binding capability of the braided tube as a surgical instrument, i.e., the maximum holding force here. However, the friction distribution between the tube and the object was ignored, making the analysis less accurate, and even out of work at some situations. Here, the friction distribution is analyzed with infinitesimal calculus, and the braided gripper is regarded as a combination of independent helical springs. According to Jedwab and Clerc [27], when the gripper is tensioned longitudinally (shown in Fig. 4(a)), the tension force on the gripper can be calculated as

$$T = 2n[\frac{2GI}{K_3}(\frac{2\sin\beta'}{K_3} - K_1) - \frac{EI\tan\beta'}{K_3}(\frac{2\cos\beta'}{K_3} - K_2)] \tag{4}$$

where $K_1 = \sin 2\beta / D,\ K_2 = 2\cos^2\beta / D,\ K_3 = D/\cos\beta.$ The tension force and the radial pressure (shown in Fig. 4(b)) loaded on a braided gripper are equivalent. Both the forces can elongate the gripper, and the relationship between them is also given by Jedwab and Clerc [27]:

$$P = \frac{2Tc}{D'L'\tan\beta} = \frac{2\pi}{p'^2}T \tag{5}$$

An object is successfully grasped for the friction between the gripper and the object caused by compression. Here, take a cylindrical object as an example to explain the self-forcing mechanism. As Fig. 5(a) shows, the cylindrical object is contained in the braided gripper. Left end of the gripper is fixed, and the object is forced rightwards with load F. The compression of the gripper to the object includes two components. One is caused by the deployment of the braided gripper and denoted by P_0. Diameter of the gripper gets larger to contain the object, and the elastic deformation needs to be sustained and causes the compression. The other is caused by the self-forcing mechanism and denoted by P_s. The gripper is tensioned longitudinally for the friction, and the tension force on the gripper is partly equilibrated with the increased radial force provided by the object. The increased radial force will also improve the friction in turn.

The force loaded on the object is described in Fig. 5(b). Firstly, with Eqs. (3-5), compression pressure caused by the elastic deformation of the braided gripper, i.e., the first component of the compression mentioned above P_0, can be calculated. Next, tension force on the braided gripper is focused on to analyze the self-forcing mechanism. The force at x=0 is equal to the load F for the left end of the gripper is fixed, and that at x=L is zero for the right end is hanging. For the existence of friction, the force on the gripper damps gradually to zero from x=0 to x=L. Differential equation of the force on the gripper in longitudinal direction can be established as

$$dT = -\mu(P_s + P_0)\pi D'dx \tag{6}$$

It is assumed that deformation of the gripper at the tension force is changeless, with which Eq. (5) still works, and Eq. (6) can be expressed as

$$dT = (-\mu \frac{2\pi^2 D'}{p'^2} T - P_0 \mu \pi D')dx \tag{7}$$

Integrating Eq. (7), explicit formula of the force distribution in longitudinal direction can be acquired as

$$T = \frac{P_0 p'^2}{2\pi}[(1 + \frac{2\pi F}{P_0 p'^2}) e^{-\mu \frac{2\pi^2 D'}{p'^2} x} - 1] \tag{8}$$

According to Eq. (8), T damps to 0 along longitudinal direction. When the object is to slide, the force at $x=L$ is just to exceed 0. As a result, the holding force when the object is to slide can be determined as

$$F_{\max} = \frac{P_0 p'^2}{2\pi}(e^{\frac{2\pi^2 \mu D' L_{\text{obj}}}{p'^2}} - 1) \tag{9}$$

The large range of holding force is achieved for the compression P_s caused by the self-forcing mechanism. When the load is light and can be ignored, the self-forcing doesn't function, and only P_0 constrains the object. As a result, light and fragile/deformable objects are likely to be grasped with less damage. In this situation, holding force on the object is the minimum and can be determined as

$$F_{\min} = \pi D_{\text{obj}} L_{\text{obj}} P_0 \mu \tag{10}$$

When releasing the object, the release force can be applied to the right end of the braided gripper to force it to deploy. When the diameter of the braided gripper is forced larger than that of the object, the object can be removed easily. In this process, the force is only to overcome the P_0, guaranteeing an easy release process. The release force can be calculated as

$$F_{\text{release}} = P_0 p'^2 / 2\pi \tag{11}$$

3. Experimental setup and finite element modelling

3.1. Holding force tests

To evaluate the self-forcing mechanism of the braided gripper, holding force tests were conducted on an *Instron* 5982 testing machine. Nylon PA66 fiber, whose Young's modulus was tested to be 3498.6Mpa through tensile tests, was selected for the fabrication of the braided gripper with the 3D braiding machine. Cylindrical objects were fabricated with ABS by 3D printing. The experimental setup is illustrated in Fig. 6. The cylindrical object with a slim handle for clamping was put in the gripper previously. Compared with the inner diameter of the braided gripper, the handle was smaller in size, and had no effects on the experimental results. One end of the braided gripper was fixed with a clamp, and the other was free. The object was forced upwards by the other clamp connected to a load cell. Displacement control was applied in the experiments and the loading rate was set as 4mm/min to avoid dynamic effects. A braided gripper grasping objects with different sizes was tested, and the parameters are listed in Table 1.

3.2. Universal grasping tests

A braided gripper was fabricated and mounted on a KUKA robot arm to test the universal grasping capability, as shown in Fig. 7(a). The gripper was actuated with four tension wires tied to the gripper's free end, to achieve the gripper's deploying and bending. The actuation system is illustrated in Fig. 7(b), which contains a four-axis controller, four actuators and four stepping motors to control the wires' stressing and relaxing. The gripper will bend to the only stressed wire, and deploy at four stressed wires. With the controller, the gripper can be driven with codes. Objects with different properties were grasped with the gripper to test the capacity of universal grasping.

3.3. Finite element modelling

To understand the self-forcing mechanism of the braided gripper in more details, the holding force tests were numerically simulated using commercial finite element code Abaqus/Explicit [32]. The numerical model is shown in Fig. 8(a), in which three parts were established, including a braided gripper, twelve arc opening plates, and a cylindrical object, to model the tests. To stagger the helical track of the fibers at the intersections, sinusoidal disturbances were added in radial direction to the helixes as introduced by Alpyildiz [33]. In this study, Matlab was used as a pre-processor to build the geometrical models of the braided gripper. The element length was set with Matlab codes, after which nodes and element numbers of the braided gripper could be obtained. So, an orphan mesh part was successfully built and imported into Abaqus. Beam element, B31, was used to mesh the gripper. Both the opening plates and the objects were modelled with shell elements and set as rigid bodies. The objects were partitioned and set with different surface properties. The first part was frictional with a coefficient of 0.2, whereas the last one was frictionless, which had no effects on the holding force, and was only used as guiding part to guarantee the convergence of the numerical analysis.

Two analysis steps were defined to model the testing process. The first step (shown in Fig. 8(b)) was to deploy the gripper. In this step, the object was inactive, and the arc opening plates moved in radial direction to deploy the braided gripper to contain the object. The second step (shown in Fig. 8(c)) was to test the maximum holding force, in which the opening plates were removed, and the object was activated. A prescribed displacement was assigned to the free DOF of the object to control its movement in longitudinal direction, and smooth amplitude definition built in Abaqus was assigned to control the rate.

According to convergence tests prior to the analysis, mesh size of 0.2mm for the braided gripper, and step times of 0.02s, and 0.1s for the two steps, respectively, yielded satisfactory results. Displacement and reaction force of the object were recorded during the analysis.

4. Results and discussions

4.1 Self-forcing mechanism of the braided gripper

Experiments and numerical simulations of a gripper grasping objects with different sizes were studied to demonstrate the self-forcing mechanism. The experiments were respectively conducted three times to each object, and the repeated results showed great consistence. The experimental force versus displacement curves are presented in Fig. 9(a-c). Comparing the three experimental curves, it is obvious that for the same gripper, the maximum holding force is much greater for a larger object. Besides, it can be seen that the reaction force increases quickly at first, and then varies periodically. In the first step, no sliding between the gripper and the object appears, and the displacement is for the elongation of the gripper. When the force increases and exceeds the holding capacity of the gripper, sliding appears. As for the waved inner surface of the braided gripper, the force has to drop sharply, and then increases gradually. The mesh configuration of the braided gripper is regular, so that the curves vary periodically. Numerical results are also drawn in the same figure, and the curves show the same tendency with the experimental ones. Forces at the crests were recorded and the error bars representing the extrema are shown in Fig. 9(d). Average of the forces are calculated as the maximum holding force and listed in Table 2. Average error between the experimental and the numerical results is 14.38%. Also, theoretical results calculated with Eq. (9) are obtained, and the error between the experimental and the theoretical results is 14.82%. Minimum holding forces

of the three objects are theoretically calculated to be 1.18N, 3.32N and 4.98N, respectively, which are respectively only 67.8%, 57.8%, and 45.1% of their theoretical maximum holding force, validating the large range of the holding force.

4.2 Effects of design parameters on the maximum holding force

The minimum holding force is caused by the elastic deformation of the gripper. The maximum holding force is derived from the self-forcing mechanism, and of more sophistications and significances. To investigate the effects of the parameters on the maximum holding force of the braided gripper, a set of numerical models were built and analyzed. All the gripper had the same length of 120mm and diameter of 20mm. Nylon material with Young's modulus 3498.6Mpa was still adopted. Other design parameters were varied and divided into two groups. One was the properties of the gripper, including d, n and β. The other was the properties of the object, including L_{obj}, D_{obj} and μ. The varied parameters of the models are listed in Table 3. The maximum holding forces are numerically analyzed and theoretically calculated with Eq. (9), and the results are presented in Fig. 10 and Fig. 11.

First, the effects of the gripper's properties are numerically analyzed with models in Group A, B and C, respectively for d, n and β, and the results are shown in Fig. 10. It can be seen from Fig. 10(a) that the force increases sharply with d. The force is 0.44N at d=0.6mm, whereas 14.4N at d=1.2mm. This is caused by the improvement of the strength of the gripper, which is linear with $I=\pi d^4/64$ according to Eq. (4). A larger gripper strength guarantees a higher compression at the same deformation, also a higher holding force. Another two parameters affect the holding capability with the same mechanism. According to Eq. (4), the strength of the gripper is positively correlated to n, whereas

negatively correlated to β within the range studied here. This is also the case of the holding capability as shown in Fig. 10(b) and Fig. 10(c). Theoretical results calculated with Eq. (9) are also drawn in Fig. 10, which show great consistence with the numerical results and validate the accuracy of the numerical analysis.

Subsequently, the effects of the properties of the object are numerically investigated with models in Group D, E and F, respectively for D_{obj}, L_{obj} and μ, and the results are presented in Fig. 11. As can be seen from Fig. 11(a), the force increases sharply with D_{obj}. This is mainly caused by the higher compression at larger deformation of the gripper. Besides, effects of L_{obj} length and μ are respectively presented in Fig. 11(b) and Fig. 11(c). It can be seen that the force increases with L_{obj} and μ, and the tendency is nearly the same. This is owing to the increase of friction, and consistent with Eq. (9). Theoretical results are also obtained with Eq. (9) and presented in Fig. 11, which show great consistence with the numerical results.

4.3 Grasping objects with different properties

A braided gripper with a length of 200mm and an inner diameter of 18mm was fabricated and mounted on a KUKA robot arm to grasp different objects. The gripper was made of 22 nylon fibers, and only weighed 7g. According to Eqs. (9~11), the maximum holding force, the minimum holding force and the release force on each wire are respectively 4.78N, 2.76N and 0.76N, while grasping a tubular object with a length of 50mm, a diameter of 50mm at a friction coefficient of 0.3. It shows a powerful grasping, a great force adaptivity and an easy release. The grasping procedure is described with Fig. 12(a-d). Its normal state is as Fig. 12(a) shows. To contain the object, it needed to deploy at the action of the four transmission wires (See Fig. 12(b)). Next, moved the robot arm to contain the object as Fig. 12(c) shows. Relaxed the transmission wires, the

gripper covered the surface of the object tightly, achieving grasping. Moved the robot arm, and the object was lifted as Fig. 12(d) shows.

Grasping fragile and deformable objects is always a great challenge, and grasping tests were first conducted to a fragile grape and a deformable jelly, and their grasping results are presented in Fig. 12(e) and Fig. 12(f), respectively. For the self-forcing mechanism, the objects were successfully grasped without damage for no excessive holding force. In addition, the experiments showed the gripper could form a circular profile with a diameter of 60mm, facilitating grasping the objects that could be contained no matter the contacting surface was smooth or angular, and the maximum weight among the grasped object reached 350g. The grasping tests further verify the great grasping capability.

4.4 Discussions

Analysis above validates the self-forcing mechanism of the braided gripper, for which the holding force is enhanced with the increase of the load. With the mechanism, greater holding force can be exerted while the gripper grasping heavy objects, guaranteeing the successful rate of grasping. As comparison, no excessive force is exerted while the gripper grasping the fragile and deformable objects, which reduces the damage rate greatly. This superiority would greatly facilitate grasping heavy rigid objects and light and fragile/deformable objects. Besides, the great deployable ratio contributes to grasping objects with various shapes and sizes. The braided gripper also exerts superiorities in other aspects. It has great design tailorability, i.e., many design parameters, including D, n, d, β and E, can be tuned to obtain a suitable mechanical properties of the gripper for actual engineering application. Besides, it is low-cost, easy-fabricated and lightweight, making it very economic. However, similar to other grippers,

the braided gripper may suffer from some difficulties in some special occasions. First, grasping sheet object is a great challenge for the small object thickness. Tiny granular object is also difficult to grasp for its limited size, and object with smooth surface is also a difficulty.

5. Conclusion

In this paper, self-forcing mechanism of the braided tube is systematically analyzed. With the self-forcing mechanism, the holding force is enhanced with the increase of the load, which facilitates grasping objects with different properties of the braided tube as the universal gripper. Taking cylindrical object as an example, the self-forcing mechanism is theoretically analyzed and explicit formulas are established for holding force range based on the open-coiled spring theory. Experimental tests and numerical simulations are also conducted to understand the self-forcing mechanism. The results show the great capability of self-forcing of the braided gripper, and a 1.2 times holding force increment is obtained for the self-forcing. Besides, a parametric analysis has been conducted with both numerical and theoretical methods. It has found that the properties of both the gripper and the object are effective to the grasping capability of the gripper. A stronger gripper with larger fiber number, larger fiber diameter, smaller braiding angle, and a rough object with larger size, are benefit to achieving a more powerful grasping. Finally, a braided gripper is fabricated and mounted on a KUKA robot arm, and successfully grasps a fragile grape and a deformable jelly, validating its great grapsing capability. Altogether this work shows that the braided tube has great potential as a robotic gripper. In the future, improving the adaptability of the braided gripper in some special occasions, such as grasping the sheet object and smooth object, is the focus. Besides, transmission system will also be improved for an easy grasping at a bent configuration.

FUNDING

This work was supported by the National Natural Science Foundation of China (Grant 51475323), the National Key R&D Program of China (Grant No. 2017YFC0110401) and the National Natural Science Foundation of China (Grant 51575377, Grant 51721003 and Grant 51520105006)

NOMENCLATURE

d	diameter of the fiber
n	number of the fiber
β	braiding angle
D	diameter of the gripper
L	length of the gripper
p	pitch of the gripper
c	number of the coils of the gripper
D_{i}	inner diameter of the gripper
D_{o}	outer diameter of the gripper
l	fiber length
T	tension force on the gripper
P	radial pressure on the gripper
E	Young's modulus of the fiber

G	rigidity modulus of the fiber
I	moment of inertia of the fiber
D_{obj}	diameter of the object
L_{obj}	length of the object
F	longitudinal load
P_0	radial pressure caused by the elastic deformation
P_s	radial pressure caused by the self-forcing mechanism
μ	friction coefficient
F_{max}	maximum of the holding force
F_{min}	minimum of the holding force
$F_{release}$	release force

REFERENCES

[1] Chen F. Y., 1982, "Force analysis and design considerations of grippers," Ind. Robot., **9**(4), pp. 243-249.

[2] Birglen L., and Schlicht T., 2018, "A statistical review of industrial robotic grippers," Robot. Cim-int. Manuf., **49**, pp. 88-97.

[3] Rus D., and Tolley M. T., 2015, "Design, fabrication and control of soft robots," Nature, **521**(7553), pp. 467-475.

[4] Shintake J., Cacucciolo V., Floreano D., and Shea H., 2018, "Soft robotic grippers," Adv. Mater., **30**(19), p. e1707035.

[5] Seguna C. M., and Saliba M. A., 2001, "The mechanical and control system design of a dexterous robotic gripper," IEEE International Conference on Electronics, St Julians, Malta, Sept. 02-05, pp. 1195-1201.

[6] Xu Z., and Todorov E., 2016, "Design of a highly biomimetic anthropomorphic robotic hand towards artificial limb regeneration" IEEE International Conference on Robotics and Automation, Stockholm, Sweden, May 16-21, pp. 3485-3492.

[7] Pons J. L., Ceres R., and Pfeiffer F., 1999, "Multifingered dextrous robotics hand design and control: a review," Robotica, **17**(6), pp. 661-674.

[8] Ilievski F., Mazzeo A. D., Shepherd R. F., Chen X., and Whitesides G. M., 2011, "Soft robotics for chemists," Angew. Chem. Int. Edit., **123**(8), pp. 1930-1935.

[9] Yamaguchi A., Takemura K., Yokota S., and Edamura K., 2012, "A robot hand using electro-conjugate fluid: Grasping experiment with balloon actuators inducing a palm motion of robot hand," Sensor. Actuat. A-Phys., **174**(1), pp. 181-188.

[10]Ma R. R., Odhner L. U. and Dollar A. M., 2013, "A modular, open-source 3D printed underactuated hand," IEEE International Conference on Robotics & Automation, Karlsruhe, Germany, May 06-10, pp. 2737-2743.

[11]Catalano M. G., Grioli G., Farnioli E., Serio A., Piazza C., and Bicchi A., 2014, "Adaptive synergies for the design and control of the Pisa/IIT SoftHand" Ind. Robot., **33**(5), pp. 768-782.

[12]Schaler E. W., Ruffatto D., Glick P., White V., and Parness A., 2017, "An electrostatic gripper for flexible objects," IEEE/RSJ International Conference on Intelligent Robots and Systems, Vancouver, Canada, Sept. 24-28, pp. 1172-1179.

[13]Shintake J., Rosset S., Schubert B., Floreano D., and Shea H., 2016, "Versatile soft grippers with intrinsic electroadhesion based on multifunctional polymer actuators," Adv. Mater., **28**(2), pp. 231-238.

[14]Amend J. R., Brown E., Rodenberg N., Jaeger J. M., and Lipson H., 2012, "A positive pressure universal gripper based on the jamming of granular material," IEEE T. Robot., **28**(2), pp. 341-350.

[15]Wei Y., Chen Y., Ren T., Chen Q., Yan C., Yang Y., and Li Y., 2016, "A novel variable stiffness robotic gripper based on integrated soft actuating and particle jamming," Soft Robot., **3**(3), pp. 134-143.

[16]De B. M., Van C. S., Mortier P., Van L. D., Van I. R., Verdonck P., and Verhegghe B., 2009, "Virtual optimization of self-expandable braided wire stents," Med. Eng. Phys., **31**(4), pp. 448-453.

[17]Hu J., 2008, "Introduction to three-dimensional fibrous assemblies," 3-D fibrous assemblies: properties, applications and modelling of three-dimensional textile structures. Woodhead Publisher, Cambridge, UK, pp. 1-32.

[18]Rial D, Tiar A, Hocine K, Roelandt J. M., and Wintrebert E., 2015, "Metallic Braided Structures: The Mechanical Modeling," Adv. Eng. Mater., **17**(6), pp. 893-904.

[19]Harte A. M., Fleck N. A., and Ashby M. F., 2000, "Energy absorption of foam-filled circular tubes with braided composite walls," Eur. J. Mech. A-Solid, **19**(1), pp. 31-50.

[20]Seok S, Onal C D, Cho K J, Wood R.J., Rus D., and Kim S., 2013, "Meshworm: a peristaltic soft robot with antagonistic nickel titanium coil actuators," IEEE-ASME T. Mech., **18**(5), pp. 1485-1497.

[21]Boxerbaum A. S., Shaw K. M., Chiel H. J., and Quinn R. D., 2012, "Continuous wave peristaltic motion in a robot," Int. J. Robot. Res., **31**(3), pp. 302-318.

[22]Heller L., Vokoun D., Šittner P., and Finckh H., 2012, "3D flexible NiTi-braided elastomer composites for smart structure applications," Smart Mater. Struct., **21**(4), pp. 317-321.

[23]Santulli C, Patel S I, Jeronimidis G, Davis F. J., and Mitchell G.R., 2005, "Development of smart variable stiffness actuators using polymer hydrogels," Smart Mater. Struct., **14**(2), pp. 434-440.

[24]Yuksekkaya M. E., and Adanur S., 2009, "Analysis of polymeric braided tubular structures intended for medical applications," Text. Res. J., **79**(2), pp. 99-109.

[25]Maetani I., Shigoka H., Omuta S., Gon K., and Saito M., 2012, "What is the preferred shape for an esophageal stent flange?," Digest. Eendsc., **24**(6), pp. 401-406.

[26]Wahl A. M., 1963, "Open-coiled helical springs with large deflections", Mechanical spring. McGraw-Hill, Berlin, Germany, pp. 241-254.

[27]Jedwab M. R., and Clerc C. O., 1993, "A study of the geometrical and mechanical properties of a self-expanding metallic stent theory and experiment," J. Appl. Biomater., **4**(1), pp. 77-85.

[28]Wang R., and Ravichandar K. 2004, "Mechanical response of a metallic aortic stent—Part I: pressure-diameter relationship," J. Appl. Mech., **71**(5), pp. 697-705.

[29]Ni X. Y., Pan C. W., and Prusty B. G., 2015, "Numerical investigations of the mechanical properties of a braided non-vascular stent design using finite element method," Comput. Method. Biomec., **18**(10), pp. 1117-1125.

[30]Kim J. H., Kang T. J., and Yu W. R., 2008, "Mechanical modeling of self-expandable stent fabricated using braiding technology" J. Biomech., **41**(15), pp. 3202-3212.

[31]Li J., Zhang Z., Wang S., Shang Z., and Zhang G., 2018, "A specimen extraction instrument based on braided fiber tube for natural orifice translumenal endoscopic surgery," ASME J. Med. Devices, **12**(3), pp. 031108.

[32]Abaqus Analysis User's Manaul, 2014, Abaqus documentation version 6.14-1, dassault systems SIMULA Corp. Providence, RI, USA.

[33]Alpyildiz T., 2012, "3D geometrical modelling of tubular braids," Text. Res. J., **82**(5), pp. 443-453.

Figure Caption List

Fig. 1 Geometry of the braided gripper.

Fig. 2 Grasping procedure of the braided gripper: (a) the normal state; (b) deployment of the gripper; (c) containing the object; (d) lifting the object

Fig. 3 Spreading of a helical fiber in plane.

Fig. 4 Elongation of a braided gripper at (a) tension force and (b) radial pressure.

Fig. 5 (a) Schematic and (b) force diagram of the gripper's grasping

Fig. 6 Experimental setup of holding force tests

Fig. 7 (a) The braided gripper mounted on a KUKA robot arm; (b) Actuation system.

Fig. 8 Finite element model: (a) Assembly of the model; (b) Deploying of the gripper with opening plates; (c) Moving the object in longitudinal direction

Fig. 9 Experimental and numerical displacement versus force curves of the gripper grasping objects with (a) D_{obj}=19.8mm, L_{obj}=20mm, (b) D_{obj}=21.8mm, L_{obj}=20mm, and (c) D_{obj}=21.8mm, L_{obj}=30mm

Fig. 10 Effects of the properties of the gripper: (a) fiber diameter; (b) fiber number; (c) braiding angle

Fig. 11 Effects of the properties of the object: (a) object diameter; (b) object length; (c) friction coefficient

Fig. 12 The braided gripper (a) in the normal state; (b) in the deployed state; (c)

contains the object; (d) lifts the object; (e) grasps the grape; (f) grasps the jelly.

Table Caption List

Information Regarding Figures and Tables

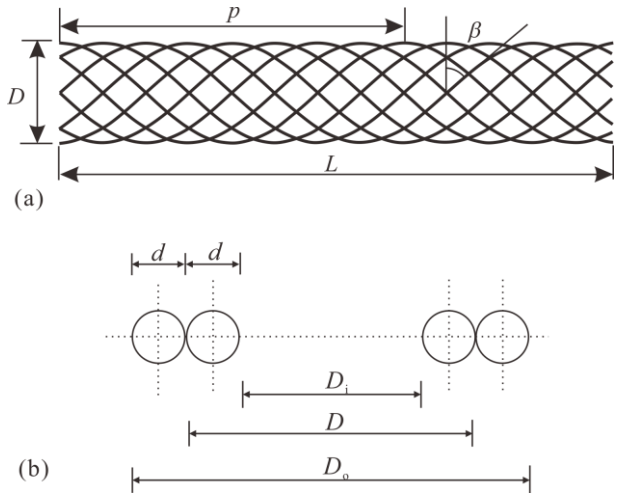

Fig. 1 Geometry of the braided gripper.

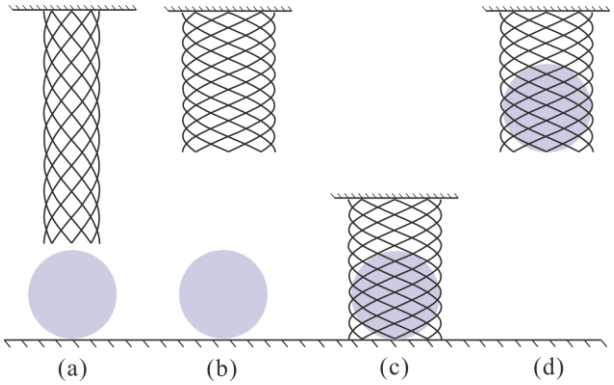

Fig. 2 Grasping procedure of the braided gripper: (a) the normal state; (b) deployment of the gripper; (c) containing the object; (d) lifting the object

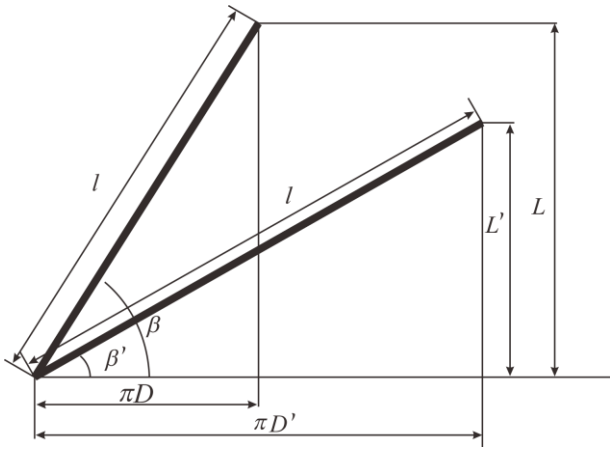

Fig. 3 Spreading of a helical fiber in plane.

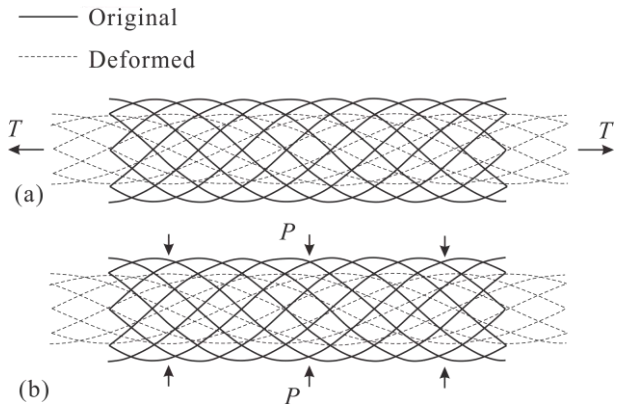

Fig. 4 Elongation of a braided gripper at (a) tension force and (b) radial pressure.

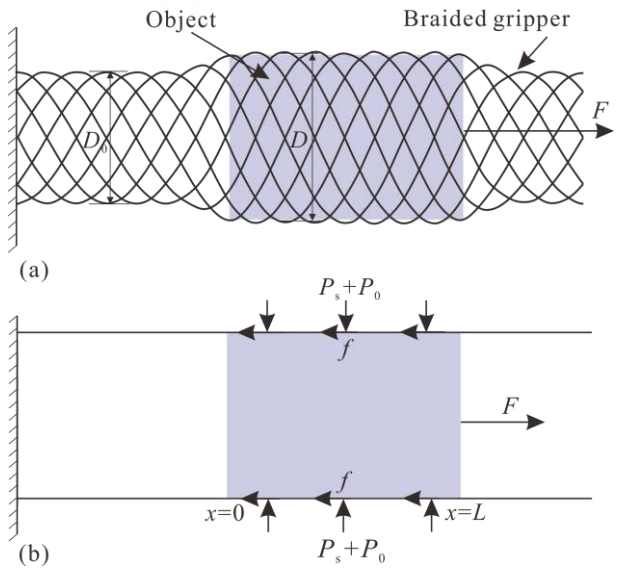

Fig. 5 (a) Schematic and (b) force diagram of the gripper's grasping.

Fig. 6 Experimental setup of the holding force tests.

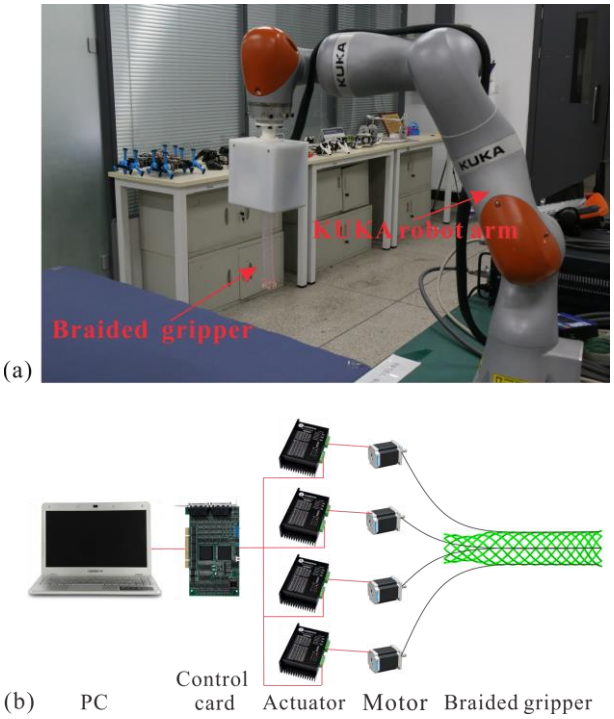

Fig. 7 (a) The braided gripper mounted on a KUKA robot arm; (b) Actuation system.

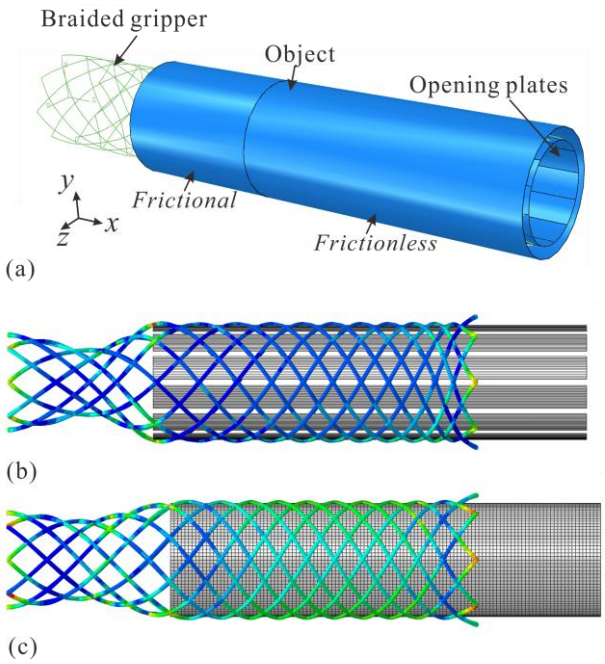

Fig. 8 Finite element model: (a) Assembly of the model; (b) Deploying of the gripper with opening plates; (c) Moving the object in longitudinal direction.

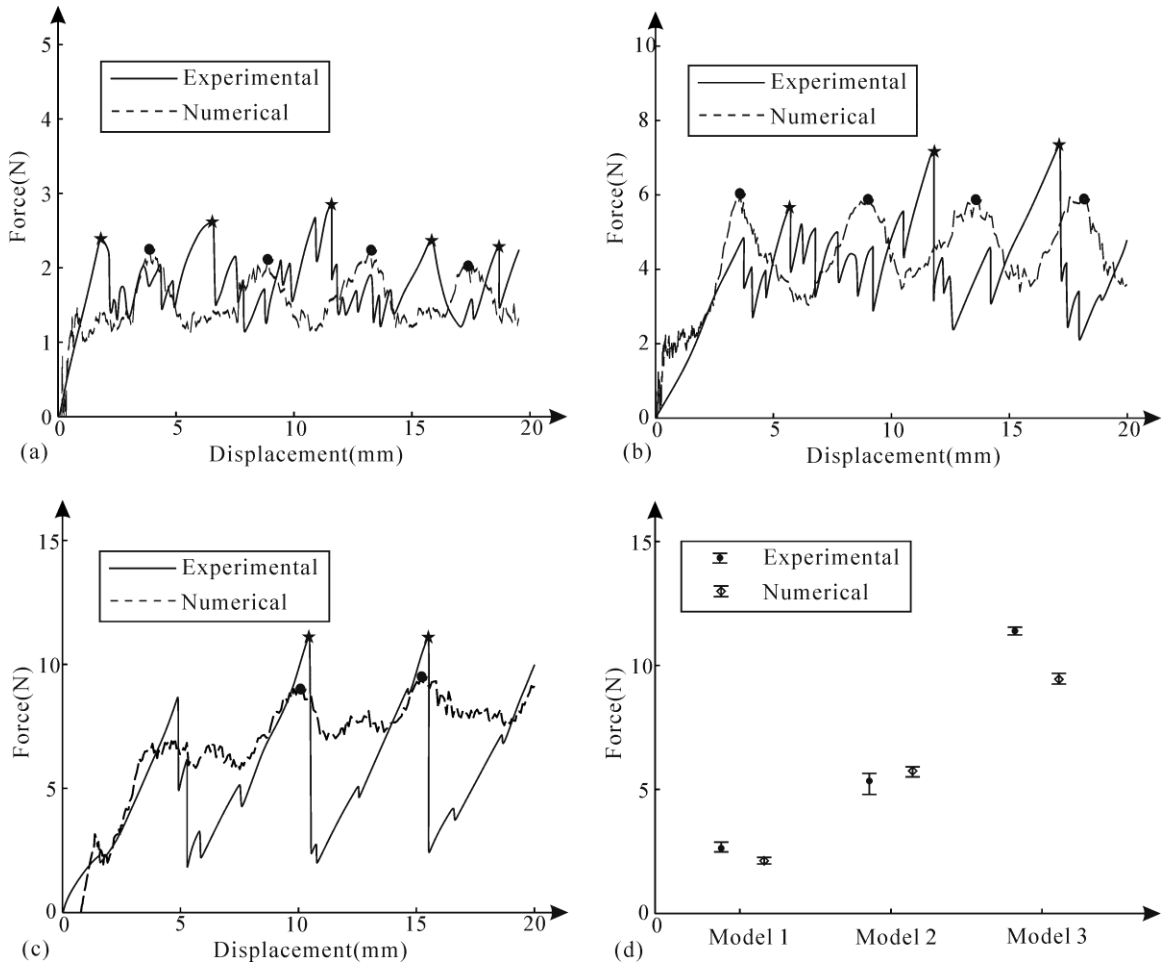

Fig. 9 Experimental and numerical displacement versus force curves of the gripper grasping objects with (a) D_{obj}=19.8mm, L_{obj}=20mm, (b) D_{obj}=21.8mm, L_{obj}=20mm, and (c) D_{obj}=21.8mm, L_{obj}=30mm, and (d) their error bars representing extrema

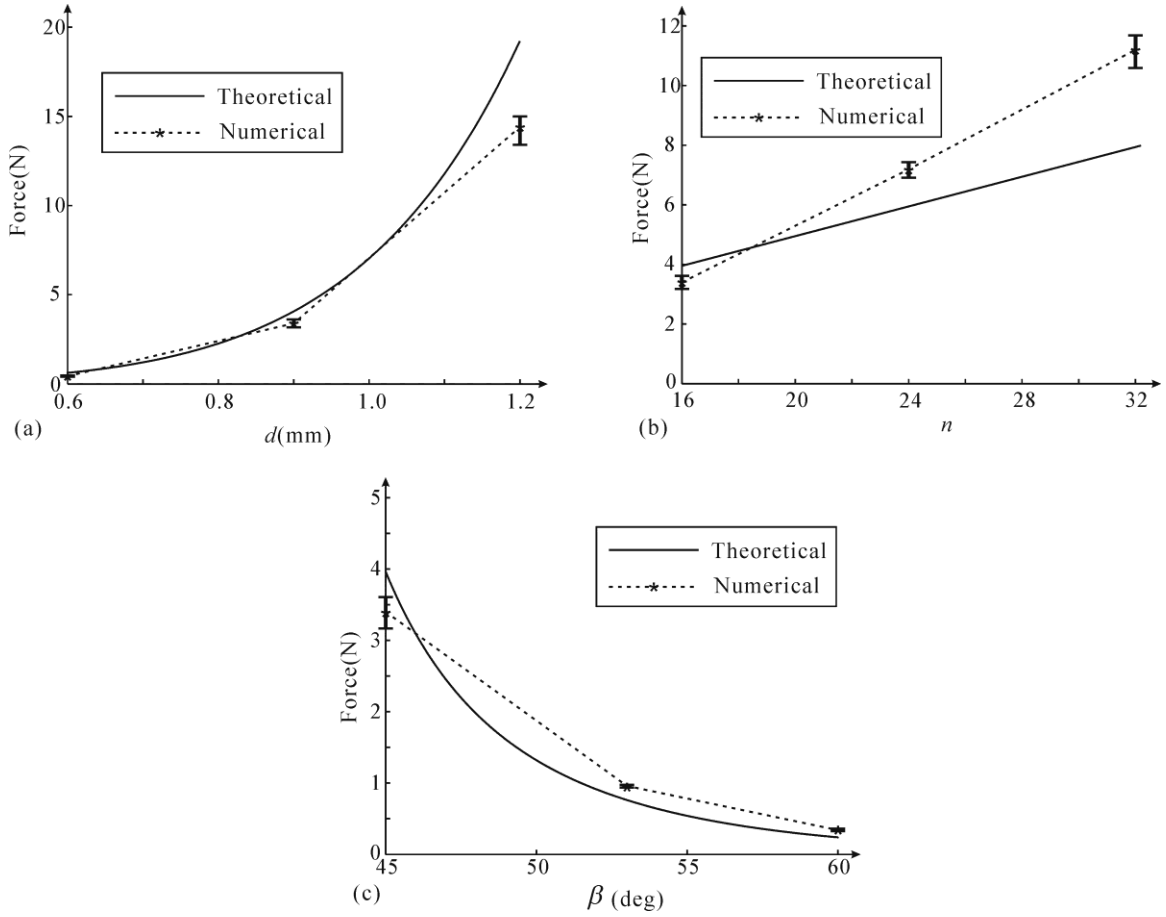

Fig. 10 Effects of the properties of the gripper: (a) fiber diameter; (b) fiber number; (c) braiding angle

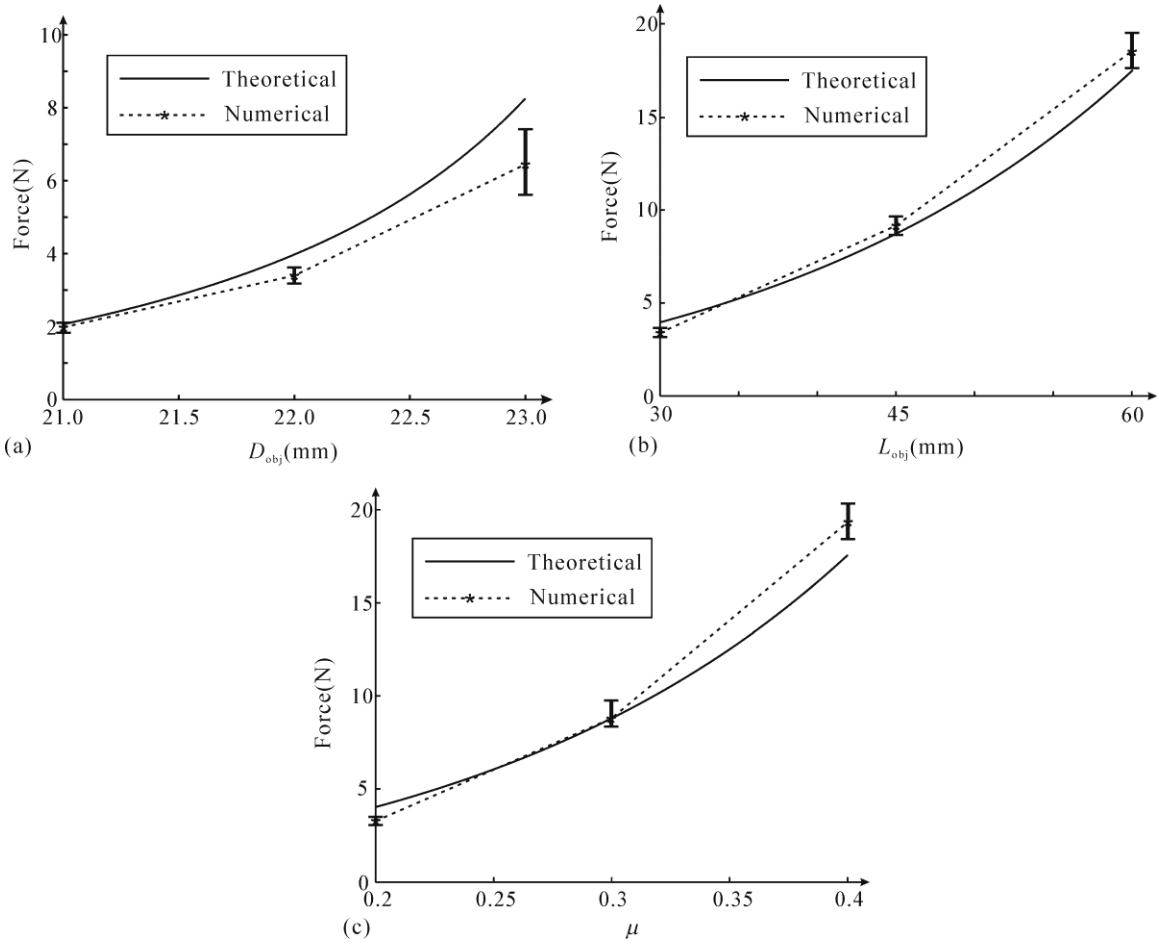

Fig. 11 Effects of the properties of the object: (a) object diameter; (b) object length; (c) friction coefficient

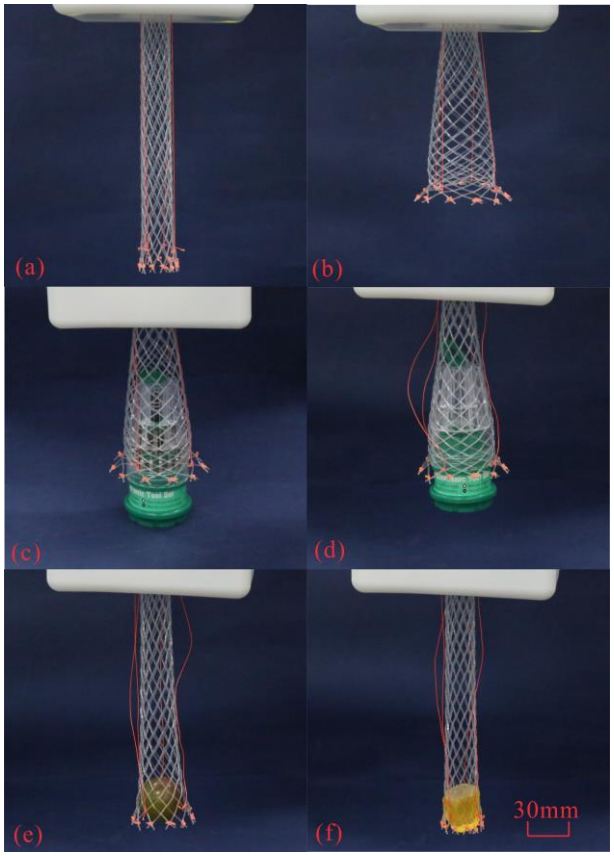

Fig. 12 The braided gripper (a) in the normal state; (b) in the deployed state; (c) contains the object; (d) lifts the object; (e) grasps the grape; (f) grasps the jelly.

Table 1 Parameters of the experimental models

Number	n [mm]	d [mm]	p [mm]	D_o [mm]	D_{obj} [mm]	L_{obj} [mm]
1					19.80	20.00
2	16	1.07	63.60	21.86	21.80	20.00
3					21.80	30.00

Table 2. Results of the maximum holding force

Models	Experimental	Numerical	Theoretical
D_{obj}=19.8mm, L_{obj}=20mm	2.64N	2.15N	1.74N
D_{obj}=21.8mm, L_{obj}=20mm	5.35N	5.75N	5.74N
D_{obj}=21.8mm, L_{obj}=30mm	11.40N	9.45N	11.05N

Table 3. Parameters of the numerical models

Group	d [mm]	n	β [°]	D_{obj} [mm]	L_{obj} [mm]	μ
A	0.6,0.9,1.2	16	45	22	30	0.2
B	0.9	16,24,32	45	22	30	0.2
C	0.9	16	45,53,60	22	30	0.2
D	0.9	16	45	21,22,23	30	0.2
E	0.9	16	45	22	30,45,60	0.2
F	0.9	16	45	22	30	0.2,0.3,0.4